

Geometrical Isomerism and Stability of Mono- and Dichalcogenide Analogs of Carbamic Acid $H_2NC(=X)YH$ (X, Y = O, S, Se)

Damanjit Kaur,* Rupinder Preet Kaur, and Pushwinder Kaur

Department of Chemistry, Guru Nanak Dev University, Amritsar 143005, India

Received February 23, 2006; E-mail: damanjit32@yahoo.co.in

Activation barriers for geometrical isomerism and tautomerization have been studied for carbamic acid and its mono- and dichalcogenide analogs at B3LYP/6-31+G*, MP2/6-31+G*, and G2MP2 theoretical levels. The studies indicate that carbamic acid with higher chalcogen prefers chalcogen at the chalcogenol position. Proton affinities, gas-phase acidities and atomic charges for these molecules have also been evaluated. Unimolecular, bimolecular, and two-step pathways for the decomposition of carbamic acid and its analogs are also analyzed, from which it was concluded that the two step mechanism is the more plausible pathway.

Carbamic acid (H_2NCOOH) has remained an elusive compound because it breaks down immediately to carbon dioxide and amine; however, its presence has been detected by IR at low temperature.[1] Amino acids containing $–NH_2$ and –COOH groups are well known stable compounds. Because of this, carbamic acid is important in biochemical studies of amino acids. Carbamic acid and its isoelectronic analog acetic acid have chemical constituents ($CO_2 + NH_3$ and $CO_2 + CH_4$) in a 1:1 ratio. There are only limited number of reports where carbamic acids could be separated. Dibenzyl substituted carbamic acid has been isolated and characterized by X-ray studies. The instability of carbamic acid is due to its tendency to undergo decarbonation under reduced pressure of CO_2 or deprotonation in the presence of an amine. In spite of its instability, it is recognized as an important intermediate in bioprocesses. The biosynthesis of carbonyl phosphate has been suggested to proceed through the fixation of carbon dioxide and ammonia with carbamic acid as intermediate,[2] and carbamic acid has been suggested as an important intermediate in the decomposition of ammonium carbamate.[3]

The esters of carbamic acids have various applications. They are valuable synthetic intermediates and act as protective groups for amines. Biologically, they are used as insecticides,[4] pesticides,[5] as antifungal and antibacterial agents,[6] as antiparasitic agent due to their antimitotic action,[7] as antiproliferative agents in vitro, as antitumor agents in vivo,[8] as inhibitory factor for fatty acid amide hydrolase activity, which is involved in deactivation of fatty acid ethanol amides.[9] Replacement of the oxygen atoms by sulphur atoms changes its inhibitory potential. Dithiocarbamates (DTCs) are important therapeutic and industrial chemicals that are released in high quantities into the environment and exhibit complex chemical and biological activities.[10] DTCs are widely used as fungicides,[11] antibacterial[12] and antidermatophytic[13] agents. Especially pyrrolidine dithiocarbamate (PDTC) has inhibitory effect on multiplication of HRV,[14] acts as antioxidant and has the capacity to inhibit the activation of NF-κB, which is a transcriptional activator important for the activation expression of HIV-1[15–17] in several biological systems. PDTC is currently advocated for use as a chemotherapeutic drug in treatment of human malignancies, such as colorectal cancer.[18] DTCs have a strong chelating capacity and prevents Cd intoxication in the liver and kidneys.[19] Diethyl carbamate, a potent free radical scavenger, has been found to prevent selenite-induced opacity in cultured rat lenses.[20] Selenocarbamates act as antiviral agents[21] and as effective superoxide anion scavenger in vitro.[22] Carbamate insecticides exert neurotoxic effects by inhibiting acetylcholinestrase in nerve and myoneural junctions including Parkinsonism.[23] Certain cyclic selenocarbamates like benzoselenazolinones imitate glutathione peroxide, which catalyses the reduction of a wide variety of hydroperoxides.[24] Some are also effective in inhibiting carragenin induced paw edema in rats and as an inhibitor of the passive foot anaphylaxis model. Rotation about the C–N bond in carbamates has been the center of many experimental and theoretical investigations because of their importance in large number of pharmaceutical and polymeric materials. The rotation barrier in carbamic acid[25] is less than amides by 3–4 kcal mol^{-1}, which has been explained as less delocalization of lone the pair present on the nitrogen atom owing to steric and electronic perturbation exerted by additional oxygen.

Proton affinity (PA) is a thermodynamic parameter useful for a quantitative understanding of the intrinsic properties in the absence of solvents. Many enzymatically catalyzed bioreactions, e.g., ATP hydrolysis, involve proton transfer. Furthermore, the protonation state of chemical groups, e.g., the side chain of amino acids, is fundamentally related to their biomolecular function. The available experimental methods have limitations in dealing with thermally non-volatile systems and for systems having more than one active site because only the protonation at the most active site is possible to calculate. Hence, experimental PA is limited to the most reactive site of the molecule.[26] On the other hand, theoretical methods have proven to be useful tools to calculate proton affinities at all possible active sites.[27] Knowledge of the preferred site of protonation is also of significance for the structure elucidation and reactivity of polyfunctional molecules. Mono- and dichalcogenide analogs of carbamic acid $H_2NC(=X)YH$ (X, Y = O,

Published on the web December 13, 2006; doi:10.1246/bcsj.79.1869

S, Se) have been selected for understanding their geometric isomerism and stability.

Computational Details

All of the calculations reported in the present study were carried out using Gaussian 98 program suite.[28] Full geometry optimizations were performed on each species without any symmetry constraint. Each optimized structure was characterized by frequency calculations to a minimum energy without any imaginary vibrational frequency or a transition state with one imaginary frequency. The HF/6-31+G*, B3LYP/6-31+G*, MP2/6-31+G*, and composite ab initio G2MP2 methods were employed. Our earlier results[25] on substituted amides using 6-31G*, 6-31G**, 6-31+G*, 6-311+G*, 6-311++G*, and AUG-CC-PVDZ basis sets indicated that 6-31+G* basis set can be applied without significant loss of accuracy. The zero point vibrational (ZPE) values were scaled[29] by 0.9135 at HF/6-31+G*, and these scaled ZPE values are used for corrections at MP2/6-31+G* theoretical level and by 0.9806 at B3LYP/6-31+G* levels to account for overestimation of the vibrational frequency at the level. The transition structure for tautomeric conversions were optimized for all of the above mentioned levels and characterized by one imaginary frequency.

The proton affinity of base B is defined as the negative of the enthalpy change (ΔH) of the process in equation (Eq. 1).

$$B + H^+ \rightarrow BH^+, \tag{1}$$

$$\Delta H = \Delta H_f(BH^+) - \Delta H_f(B) - \Delta H_f(H^+), \tag{2}$$

$$PA = -\Delta H = -[(E_{e(BH+)} + ZPE_{(BH+)} + H_{vib(BH+)}) - (E_{e(B)} + ZPE_{(B)} + H_{vib(B)})] + 5/2RT, \tag{3}$$

where E_e is the electronic energy, ZPE is scaled zero point energy, H_{vib} is the vibrational enthalpy correction scaled[29] by 0.8945 at the MP2/6-31+G* and 0.9989 at the B3LYP/6-31+G* theoretical level and the term $5/2RT$ includes ΔnRT ($\Delta(PV)$ for the above reaction and translational energy of the proton).

The gas-phase acidity[30] is defined as the enthalpy change of deprotonation (ΔH^{298}) for Eq. 4.

$$AH(g) \rightarrow A^-(g) + H^+(g). \tag{4}$$

The enthalpy of deprotonation, ΔH^{298}, was computed using Eqs. 5 and 6, where

$$\Delta H = \Delta E^{298} + \Delta(PV), \tag{5}$$

$$\Delta E^{298} = E^{298}(A^-) + 3/2RT - E^{298}(AH). \tag{6}$$

E^{298}(AH) and $E^{298}(A^-)$ stand for the total energies of the most stable syn conformation of acids and their anions, including the thermal energy correction at $T = 298.15$ K. In Eq. 5, we substituted $\Delta(PV) = RT$ (1 mole of gas is obtained in Eq. 4).

NBO analysis[31,32] has been used to quantitatively estimate the energy of the second-order interactions ($E^{(2)} = -2F_{ij}/\Delta E_{ij}$) ($E_{ij} = E_i - E_j$ is energy difference between the interacting molecular orbitals i and j; F_{ij} is the Fock matrix element for the interaction between i and j). To understand the observed trends in electron delocalization, MP2/6-31+G* optimizations and NBO analysis on the corresponding structure has been carried out on the $NH_2C(=X)$-YH molecules.

Molecule	X	Y
1	O	O
2	O	S
3	O	Se
4	S	S
5	S	O
6	S	Se
7	Se	Se
8	Se	O
9	Se	S

Fig. 1. **S** and **A** represent the syn and anti conformation of carbamic acid and its analogs.

Results and Discussion

Isomerism in Carbamic Acid. Full geometry optimization of carbamic acid and its chalcogenide analogs at B3LYP/6-31+G* and MP2/6-31+G* levels of theory leads to two stable ground state conformations (**S**, **A**, Fig. 1), which is in accordance with the observations made by Remko and Rode.[30] Geometrical parameters for the optimized ground state for molecules **1**–**9** are reported in Tables S1–S4 in Supporting Information. They have assigned the greater stabilization of the syn conformation over the anti conformation to intramolecular electrostatic interactions and extended conjugation which is the electron delocalization resulting from lone pairs of electrons present on N, X, and Y. The separation between X1 and H5 is reported in the Table 1 along with relative energies in order to understand importance of non-bonded interactions. Sum of van der Waals radii for the participating atoms are also included in Table 1 for comparison. The non-bonded distance X1···H5 is less than the sum of van der Waals radii clearly indicating the importance of non-bonded interactions. The sum of angles around N is 360° or close to 360° in **1**–**9** molecules (included in Tables S1 and S2) that indicates that lone pair on nitrogen is highly delocalized. The syn–anti energy differences for the molecules **1**, **5**, and **8** are significantly larger than rest of the molecules. These three molecules contain hydroxy group as proton donor. To evaluate the extent of contribution to relative energy values by these types of interactions, the relative energies of methyl esters of the corresponding acids have been determined. The methyl esters of **1**, **5**, and **8** have a syn anti energy difference of 7.99, 8.46, and 6.06 kcal mol^{-1} at B3LYP/6-31+G* theoretical level which differs by 0.04, 1.84, and 5.39 kcal mol^{-1}, respectively, from the corresponding acids. The variations are representative of intramolecular hydrogen bonding in **1** and **5** respectively. The steric interactions of CH_3 group with the bulkier Se reduces the syn–anti energy difference of methyl ester of **8**. With the absence of hydrogen-bonding interaction, the syn–anti energy difference in methyl esters of molecules **1**–**9** arises from the difference in extended conjugation, which is significantly larger than the intramolecular hydrogen-bonding interactions in parent molecules. The activation barriers for syn to anti transformation and vice versa are also included in Table 1. The activation barriers for syn → anti for **1**, **5**, and **8** are relatively greater than those for the rest of the molecules, and the barrier decreases in the order **8** > **5** > **1**. The increase in ability of accepting the charge in higher chalcogen analogs of $H_2NC(=X)$–OMe favors extended conjugation and explains the observed order. The higher activation barrier indicates loss of extended elec-

Table 1. Relative Energies (ΔE, kcal mol^{-1})[a] of Syn and Anti Conformers, Enthalpy Difference (ΔH, kcal mol^{-1})[b], Activation Barrier (kcal mol^{-1}), Non-Bonded Distance between X1 and H5 ($d_{X\cdots H}$, in Å) in Syn Conformer and Sum of van der Waals Radii between X1 and H5 (in Å)

No	Molecule	Relative energies		Activation barrier at B3LYP/6-31+G*		$d_{X1\cdots H5}$ /Å	Sum of van der Waals radii of X1 and H5/Å
		B3LYP/6-31+G* ΔE[a] (ZPE$_{corr}$)	G2MP2 ΔH[b]	Syn → Anti	Anti → Syn		
1	$H_2NC(=O)OH$	8.03	6.7	11.70	3.67	2.31	2.72
2	$H_2NC(=O)SH$	2.55	1.7	5.76	3.11	2.58	2.72
3	$H_2NC(=O)SeH$	1.30	0.9	5.29	3.98	2.70	2.72
4	$H_2NC(=S)SH$	3.04	1.4	6.57	3.94	2.85	3.00
5	$H_2NC(=S)OH$	10.30	8.3	13.58	3.28	2.60	3.00
6	$H_2NC(=S)SeH$	1.19	0.3	5.44	4.42	3.00	3.00
7	$H_2NC(=Se)SeH$	0.57	0.3	5.99	5.62	3.06	3.10
8	$H_2NC(=Se)OH$	11.45	8.8	14.39	2.95	2.68	3.10
9	$H_2NC(=Se)SH$	3.95	1.3	7.01	4.06	2.96	3.10

a) $\Delta E = E_{syn} - E_{anti} + ZPE_{corr}$. b) $\Delta H = H_{syn} - H_{anti}$.

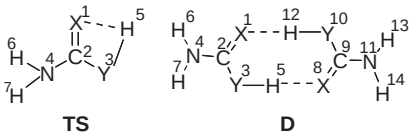

Molecule	X	Y
1	O	O
2	O	S
3	O	Se
4	S	S
5	S	O
6	S	Se
7	Se	Se
8	Se	O
9	Se	S

Fig. 2. Transition state (**TS**) for unimolecular and dimer (**D**) for bimolecular 1,3 proton transfer responsible for tautomerism.

Table 2. Relative Energies (ΔE_{taut}, in kcal mol^{-1})[a] of the Tautomeric Forms and Activation Barrier (in kcal mol^{-1}) of Tautomerization for the Unimolecular 1,3 Proton Transfer at B3LYP/6-31+G* Theoretical Level

Tautomerization	Relative energy ΔE_{taut}[a]/kcal mol^{-1}	Activation barrier ΔE/kcal mol^{-1}
$H_2NC(=O)SeH \rightleftharpoons H_2NC(=Se)OH$	1.8	29.12
$H_2NC(=O)SH \rightleftharpoons H_2NC(=S)OH$	2.5	15.46
$H_2NC(=S)SeH \rightleftharpoons H_2NC(=Se)SH$	0.38	14.77

a) $\Delta E_{taut} = E_{XY} - E_{YX} + \Delta ZPE_{(corr)}$.

tron delocalization in the transition state.

The absolute energies data for molecules **1**–**9** indicate the preference for the molecule to have a higher chalcogen as the chalcogenol, because the stability of C=X double bond decreases in the order O > S > Se. The transformation between the two forms can occur through proton transfer. Tautomerism involving transfer of a proton can occur intramolecularly or intermolecularly. The intramolecular proton-transfer pathway is the probable pathway for isolated molecules in vapor phase at very low pressure. The structure of transition state for unimolecular 1,3 proton transfer (Fig. 2) has been optimized at B3LYP/6-31+G* theoretical level to evaluate activation barriers for the tautomerization. The activation barriers are reported in Table 2. From the Table 2, the barriers range from 14.77 to 29.12 kcal mol^{-1}. The intermolecular pathway for the proton transfer has also been studied using dimeric transition state. The energies of dimerization ($\Delta G_{taut} = 2G_{monomer} - G_{dimer}$) suggest that dimers are stabilized by non-bonded interactions. The non-bonded distance X···H for the six types of dimers are reported in Table 3. These distances are less than sum of van der Waals radii of atoms suggesting strong non-bonded interactions leading to preference of dimeric state over monomeric state. The crystal structure of dibenzyl-substituted carbamic acid $[PhCH_2)_2NC(O)OH]$ suggests the presence of two end on hydrogen bonds.[33] The dimerization energies are significantly high for molecules X = S, Se and Y = O. The hydrogen attached to electronegative oxygen atoms develops a substantial positive charge, and O–H bond is known to be better hydrogen-bond donor than S–H and Se–H. As can be seen from the Table 3, the charge on hydrogen atom attached to O is relatively much higher than on other molecules. The activation energies required for 1,3 proton transfer involving dimeric transition states tautomerization are also reported in the Table 3. The barriers are significantly lower than the barriers for unimolecular proton transfer. Thus, 1,3 proton transfers through dimeric transition state in these molecules is favored over intramolecular 1,3 proton transfer and are small enough that the molecules easily undergo 1,3 proton transfer.

Acidities of Molecules. Though separation of carbamic acid has posed a challenge to the scientists, the existence of its anion and protonated[34] forms are known and are well characterized. The acidities of carbamic acid and its analogs reflect their tendency to deprotonate. The gas-phase acidities evaluated by using Eq. 4 at B3LYP/6-31+G* theoretical level and composite G2MP2 method are listed in Table 4. From the Table 4, the carbamic acid with X = Se and Y = Se is the strongest acid. The strength of acids decreases in the order Se > S > O for Y with X = Se. The order can be understood on the basis of electronegativity and concept of charge capacity introduced by Politzer et al.[35] The less electronegative selenium has a higher charge capacity than sulphur that is in turn larger than oxygen, which results in larger stabilization of anion in the order **7** > **9** > **8**. Similar orders for acidity are observed for X = S and X = O. The variation in acidity as a

Table 3. Relative Energies of Dimers (ΔG_{dtaut}, kcal mol^{-1}), Activation Barrier (kcal mol^{-1}), Non-Bonded Distance between X1 and H5 ($d_{X1\cdots H5}$, in Å), Sum of van der Waals Radii (in Å), Atomic Charge on H5 (q_{H5}) and X1 (q_{X1}) for Dimer Important for Electrostatic Interactions at B3LYP/6-31+G* Theoretical Level

No	Dimer	Relative energy ΔG_{dtaut}[a] /kcal mol^{-1}	Activation barrier (ΔG) /kcal mol^{-1}	$d_{X1\cdots H5}$ /Å	Sum of van der Waals radii of X1 and H5 /Å	q_{H5}	q_{X1}
2D	$[H_2NC(=O)SH]_2$	1.29	13.17	1.98	2.72	0.15	−0.57
3D	$[H_2NC(=O)SeH]_2$	3.82	6.76	1.93	2.72	0.22	−0.49
5D	$[H_2NC(=S)OH]_2$	1.93	5.52	2.15	3.00	0.42	−0.18
6D	$[H_2NC(=S)SeH]_2$	4.25	2.29	2.51	3.00	0.19	−0.38
8D	$[H_2NC(=Se)OH]_2$	6.13	5.89	2.24	3.10	0.43	−0.21
9D	$[H_2NC(=Se)SH]_2$	2.65	3.54	2.56	3.10	0.13	−0.12

a) $\Delta G_{dtaut} = 2G_{monomer} - G_{dimer}$.

Table 4. Gas-Phase Acidities (in kcal mol^{-1}) of Carbamic Acid and its Thio and Seleno Analogs at B3LYP/6-31+G* and G2MP2 Theoretical Level[a]

No	Molecule	B3LYP/6-31+G*	G2MP2
1	$H_2NC(=O)OH$	342.16	344.69
2	$H_2NC(=O)SH$	333.09	334.63
3	$H_2NC(=O)SeH$	330.02	329.61
4	$H_2NC(=S)SH$	324.97	327.15
5	$H_2NC(=S)OH$	328.60	331.25
6	$H_2NC(=S)SeH$	322.34	323.46
7	$H_2NC(=Se)SeH$	320.26	319.91
8	$H_2NC(=Se)OH$	325.70	325.38
9	$H_2NC(=Se)SH$	322.26	323.23

a) $\Delta E^{298} = E^{298}(A^-) + 3/2RT - E^{298}(AH)$ and $\Delta H = \Delta E^{298} + \Delta(PV)$.

function of X follows the order O < S < Se, which clearly reflects the importance of electron delocalization in stabilization of the anion, and the stabilization is strongest for X = Se. The observations also indicate the importance of extended conjugation in the stabilization of anions that increases in the order O < S < Se. The acidity of carbamic acid **1** is 342.16 kcal mol^{-1}, which is comparable to the acidity of formic acid (ΔH = 340.4 kcal mol^{-1} at B3LYP/6-311+G(d,p) level).

Proton Affinities of Molecules. High level ab initio methods (G2) and CBS methods are remarkably accurate and provide PA within 2 or 3 kcal mol^{-1} as indicated by studies of Merrill and Kass.[36] The results reported by Smith and Radom infer that G2 level reproduce experimental PA with an accuracy of 2.3 kcal mol^{-1}.[37] The molecules in the present study possess three potential basic sites X1, N4, and Y3 (atoms possessing lone pairs of electrons) that might accept protons to form either ammonium ion or chalcogenium ion. The protonation at X1 and N4 have been studied except Y3, because protonation at Y3 leads to the destabilization of the molecule and results in the breakage of C2–Y3 bond. Calculations using B3LYP/6-31+G*, MP2/6-31+G*, and G2MP2 model chemistries demonstrated that the protonation at the carbonyl X (O, S, Se) atom site yields a more stable structure than protonation at N atom and are reported in Table 5. Proton affinities at X have been evaluated for the most stable ground-state conformation and protonation at X as cis to NH_2 group. X protonation with H oriented cis to NH_2 group being more stable than the other orientations. It is the availability of lone pair on X-atom, which can easily bond with H^+ whereas lone pair on N-atom is delocalized over the molecule. Hillebrand et al. assigned the trends in proton affinities of ammonia and its derivative to the nitrogen lone pair s character, which determines the strength of binding to proton.[26] As can be seen from the Table 5, the proton affinities at X = O increase in the order of Y as O < S < Se, which clearly suggest that the stability of protonated species in addition to availability of lone pair decides the proton affinity. The proton affinity at X increases in the order O < S < Se.

Protonation at the N4 site is accompanied by shrinkage of the C2–X1 bond, whereas elongation of the C2–N4 bond occurs. When the proton binds to the lone pair on the N4-atom,

Table 5. Proton Affinities (PA, in kcal mol^{-1}) for Carbamic Acid and Its Thio and Seleno Analogs at Different Theoretical Levels

No	Molecule	B3LYP/6-31+G*		MP2/6-31+G*		G2MP2	
		At X1	At N4	At X1	At N4	At X1	At N4
1	$H_2NC(=O)$–OH	189.4	181.7	185.1	181.3	193.2	183.6
2	$H_2NC(=O)$–SH	191.2	183.6	186.6	183.2	195.6	186.0
3	$H_2NC(=O)$–SeH	193.0	185.3	188.1	184.0	196.4	187.3
4	$H_2NC(=S)$–SH	200.4	183.8	196.8	186.9	204.3	188.3
5	$H_2NC(=S)$–OH	196.6	182.7	192.5	185.1	200.6	185.9
6	$H_2NC(=S)$–SeH	202.3	185.9	197.2	187.8	204.8	188.8
7	$H_2NC(=Se)$–SeH	205.0	187.5	198.0	187.7	206.8	189.6
8	$H_2NC(=Se)$–OH	199.1	183.4	193.1	184.5	201.3	185.9
9	$H_2NC(=Se)$–SH	202.3	186.4	196.4	187.2	205.2	188.9

Table 6. Second-Order Delocalization Energy ($E^{(2)}$ in kcal mol^{-1}) and Important Lone Pair Occupancies of Carbamic Acid and Its Thio and Seleno Analogs at MP2/6-31+G* Theoretical Level for Syn Conformation

No.	Molecule	Second-order $E^{(2)}$ delocalization energies				Occupancies		
		$n_N \rightarrow \sigma^*_{X-C(1)}$	$n_N \rightarrow \pi^*_{X-C(2)}$	$n_X \rightarrow \sigma^*_{C-Y}$	$n_X \rightarrow \sigma^*_{C-N}$	ρ(2)X1	ρ(2)Y3	ρN4
1	$H_2NC(=O)OH$	19.84	28.63	42.4	28.51	1.87	1.90	1.83
2	$H_2NC(=O)SH$	12.26	40.95	37.30	29.11	1.87	1.90	1.82
3	$H_2NC(=O)SeH$	—	88.87	40.61	28.39	1.87	1.93	1.80
4	$H_2NC(=S)SH$	—	107.56	19.39	16.70	1.89	1.88	1.75
5	$H_2NC(=S)OH$	—	112.10	23.35	15.86	1.88	1.88	1.76
6	$H_2NC(=S)SeH$	—	107.18	22.54	16.19	1.88	1.90	1.75
7	$H_2NC(=Se)SeH$	—	116.36	16.99	12.70	1.90	1.88	1.74
8	$H_2NC(=Se)OH$	—	121.76	17.92	12.66	1.90	1.87	1.74
9	$H_2NC(=Se)SH$	—	116.85	15.04	12.95	1.90	1.87	1.74

breakage of the partial π-bond character between carbon and nitrogen occur. Protonation at X is accompanied by an increase in the C=X bond distance, whereas the C–N bond distance decreases and the N–C–X bond angle decreases. The elongation of the C2–X1 bond is understandable due to the shift of electron density from atom X1 toward the proton resulting in the breaking of the π-bond. Protonation at X1 results in shortening of C–N bond due to enhanced delocalization from the lone pair of the N atom in order to stabilize the protonated molecule. The proton affinity of N ranges from 183.6 kcal mol^{-1} for **1S** to 189.6 kcal mol^{-1} for **7S** molecule at G2MP2 level. The values are significantly lower than proton affinity of NH_3, 204.0 kcal mol^{-1} determined experimentally. Comparatively lower availability of the lone pair on N in **1**–**9** molecules results from the conjugation of the lone pair of electrons with rest of the molecules. The delocalization of lone pair of electrons from nitrogen is also clearly reflected by second-order stabilization energies $E^{(2)}$ evaluated by NBO analysis using MP2/6-31+G* densities of these molecules and are discussed in following section.

The protonation at X is accompanied by enthalpy change of 193.2 to 205.2 kcal mol^{-1} for molecules **1**–**9**. The proton affinities for X sites are nearly 10 kcal mol^{-1} higher than the values for N sites. The higher ability of nitrogen lone pair to delocalize its lone pair results in favors higher basicity for the X site.

Electron Delocalization. The extent of various delocalizations is represented by the second-order delocalization energies $E^{(2)}$, that are evaluated using NBO analysis. Some of the important values for second-order delocalization energies are listed in Table 6. The NBO analysis shows that the $n_N \rightarrow \pi^*_{C-X}$, $n_X \rightarrow \sigma^*_{C-N}$, and $n_X \rightarrow \sigma^*_{C-Y}$ are the important interactions which lead to the delocalization of the lone pairs present on nitrogen and both chalcogen atoms. The $n_N \rightarrow \pi^*_{C-X}$ delocalization increases in the order of Y as O < S < Se with X = O; however, the $E^{(2)}$ values are much smaller than the values for similar delocalizations in amides, e.g., the $E^{(2)}$ associated with the $n_N \rightarrow \pi^*_{C-X}$ for the molecules **1**, **2**, and **3** are 28.63, 40.95, and 88.87 kcal mol^{-1} at MP2/6-31+G*, respectively, while the corresponding delocalization in formamide has $E^{(2)}$ of 88.54 kcal mol^{-1}. In molecules **4**–**9** where X = S or Se, the $E^{(2)}$ values decrease in order of Y as O > S > Se; however, the magnitude of variation is smaller in comparison to that in **1**, **2**, and **3** (Table 6). These $E^{(2)}$ values are comparable to the values for $n_N \rightarrow \pi^*_{C-X}$ delocalization in thio (111.15 kcal mol^{-1}) and selenoamides (120.39 kcal mol^{-1}) at the same theoretical level. The presence of highly electronegative oxygen at position Y in **1**, results in an increase in ΔE_{ij} for $n_N \rightarrow \pi^*_{C-O}$ delocalization from 0.59 in formamide to 0.88 a.u. in **1**. ΔE_{ij} decreases to 0.76 and 0.57 in **2** and **3**, respectively, when Y = S and Se. $E^{(2)}$ values are inversely proportional to ΔE_{ij}. It is interesting to note that in the molecules under study, the $n_N \rightarrow \pi^*_{C-X}$ and $n_Y \rightarrow \pi^*_{C-X}$ interactions involve a shift of electrons density to the same acceptor orbital but with a change in X from oxygen to selenium through sulfur, there is an increase in $E^{(2)}$ for both the type of interactions. The trend results from a decreasing ΔE_{ij} and an increase in size of π^*_{C-X} orbital with the presence of higher chalcogen of larger size and polarizability. The decrease in $n_X \rightarrow \sigma^*_{C-N}$ and $n_X \rightarrow \sigma^*_{C-Y}$ interaction energies with X in the order O > S > Se indicates a decrease in the donor ability of the chalcogen in the higher chalcogens. This order can also explain higher affinity of higher chalcogens toward protons. The lone pair occupancies that are involved in electron delocalizations are also included in Table 6. The lone pair on the nitrogen is relatively more delocalized in comparison to those present on X and Y positions. But occupancies being lower than 2.0 which indicate the importance of chalcogens at positions X and Y in the stability of the molecules.

Charges become important criterion where electrostatic interactions are involved. Atomic charges obtained by using NBO analysis are reported in Table S5 in the Supporting Information. The carbonyl carbon in **1** with X = O and Y = O has a positive charge of 1.10 units in tune with the higher electronegativity of the two oxygen atoms attached to carbon. The charge on the carbon is reduced to approximately half when S or Se replaces one of the oxygen atoms. The charge is further reduced to an insignificant amount when at both X and Y are either S or Se. The oxygen at position X in **1** with Y = O has −0.756 units of charge that decreases to −0.717 and −0.722 with replacement of O at Y position to S and Se, respectively. The sulfur atom at position X in **5** carries a charge of −0.274. The charge density on the sulfur decreases with the presence of sulfur and selenium at position Y. Though the charge at position X is decided by the electronegativity of X, the variation in charge with change in Y suggests that electron delocalization results from the extended conjugation. The nitrogen atom is also highly charged showing only small variation with a change in chalcogen at position Y. The charge on the hydrogen

Table 7. Gibbs Free Energy for Reaction (**7**) (ΔG_1, in kcal mol^{-1}) and Reaction (**8**) (ΔG_2, in kcal mol^{-1}) for Carbamic Acid and Its Thio and Seleno Analogs at G2MP2 Theoretical Level

No	Molecule	ΔG_1/kcal mol^{-1}	ΔG_2/kcal mol^{-1}
1	$H_2NC(=O)OH$	10.52	−174.25
2	$H_2NC(=O)SH$	12.08	−175.16
3	$H_2NC(=O)SeH$	9.25	−178.37
4	$H_2NC(=S)SH$	9.80	−179.86
5	$H_2NC(=S)OH$	16.34	−171.07
6	$H_2NC(=S)SeH$	7.31	−182.69
7	$H_2NC(=Se)SeH$	4.45	−186.48
8	$H_2NC(=Se)OH$	14.58	−172.80
9	$H_2NC(=Se)SH$	9.21	−182.37

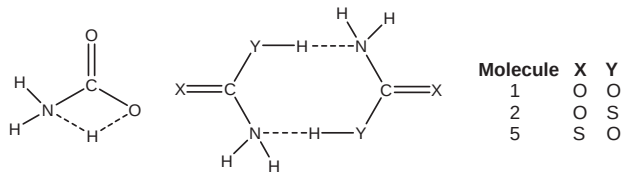

Fig. 3. (a) Transition state for unimolecular decomposition of carbamic acid. (b) Dimer for bimolecular proton transfer and C–N rupture in a concerted fashion.

atom attached to chalcogen is decided mainly by the electronegativity of the chalcogen to which it is attached.

Stability of Carbamic Acid. The ab initio calculations suggest carbamic acid molecules with a syn arrangement of YH bond with respect to C(=X) are more stable than anti for X = O, S, Se; Y = O, S, Se. The carbamic acid molecule **1** undergoes decomposition to NH_3 and CO_2 under experimental conditions. For carbamic acid, $\Delta G_1 = 10.52$ kcal mol^{-1}. The ΔG values for reaction (**8**) for X = O, S, Se and Y = O, S, Se are also given in Table 7.

$$H_2NCOOH \rightleftharpoons NH_3 + CO_2. \quad (7)$$

$$H_2NCXYH \rightleftharpoons NH_3 + CXY. \quad (8)$$

The ΔG values clearly suggest that molecules **1**–**9** are thermodynamically less stable molecules. The transition state (see Fig. 3) for H atom transfer from hydroxy group to amino group has been also optimized at B3LYP/6-31+G* level. This transfer has an energy barrier of 33.30 kcal mol^{-1} at 0 K in the gas phase. The high barrier suggests kinetic stability for unimolecular decomposition of carbamic acid. Similar transition states for the molecules **2**–**9** could not be optimized since these molecules involve either weak hydrogen-bond donors (Y–H; Y = S, Se) or weak hydrogen-bond acceptors (X = S, Se). Studying the kinetics and mechanism of the reversible dissociation of ammonium carbamate, Ramachandran et al.[3] analyzed three proposed mechanisms. Two mechanisms involve a carbamic acid as intermediate. They consider unimolecular decomposition impossible because of a high activation barrier. In the second mechanism, the activation barrier is reduced considerably with the involvement of second NH_3 molecule in the transition state. A third mechanism is proposed to occur in the solid state only. Intermolecular electrostatic interactions play an important role in molecules possessing high charge separations leading to dimer formation. Our attempts to optimize such dimers where proton transfer and C–N bond rupture can occur in concerted fashion succeeded only in **1**, **2**, and **5** (see Fig. 3). These dimers lead to stabilization, and thus, the activation barrier is lower by 4.14, 6.70, and 4.74 kcal mol^{-1} respectively. The attempts to optimize remaining six dimers failed. Dimerization is not a simple consequence of electrostatic interactions but rather is consequence of weak hydrogen-bond formation resulting from $n_N \rightarrow \sigma^*_{O-H}$ electron delocalization that requires change in hybridization at the N, which is apparent from the H–N–H bond angles. Dimerization in molecules **3**, **4**, **6**, **7**, **8**, and **9** requires a loss in the stabilization energy associated with $n_N \rightarrow \pi^*_{C-X}$ delocalization, which is comparatively higher in these molecules (Table 6), and it is a well accepted fact that the hydrogen bond donor ability of Y–H bond decreases in the order O > S > Se.

Two-step mechanism for the decomposition of carbamic acid and its analogs through protonation at N followed by C–N bond rupture has also been considered.

$$NH_2C(=X)YH + H^+ \rightarrow N^+H_3C(=X)YH,$$

$$N^+H_3C(=X)YH \rightleftharpoons NH_3 + CXY + H^+. \quad (9)$$

ΔG_2 values for reaction (**9**) are also listed in Table 7, and they values clearly suggest that the two-step mechanism is plausible in the presence of H^+. The presence of water molecules that can act as acid as well as base can catalyze the decomposition process. Though unimolecular decomposition of carbamic acid seems improbable due to high activation barrier, the gas-phase acidities indicate that these molecules have high tendency to lose a proton in the presence of a proton acceptor. Carbamic acids are good proton acceptors as suggested by proton affinity values. The reports by Masuda et al.[38] and Rudkevich and Xu[39] for the formation of carbamic acid by bubbling CO_2 through a solution of amines in protophilic highly dipolar aprotic solvents support our results that H^+-catalyzed decomposition is the most probable pathway.

Conclusion

Carbamic acid molecules have been predicted to be stable molecules in the gas phase, and they undergo tautomerization with activation barriers ranging from 0.76 to 1.75 kcal mol^{-1} in **1**–**9** molecules with higher chalcogen occupying the –ol position. As well, the activation barrier for gas-phase unimolecular decomposition is considerably high. Unimolecular, bimolecular, and a two-step mechanism for decomposition of carbamic acid and its analogs were studied, and out of the three, the two-step hydrogen ion-catalyzed decomposition followed C–N bond rupture is found to more plausible.

The authors are thankful to Council of Scientific and Industrial Research (CSIR), New Delhi, for the financial assistance in the present research work.

Supporting Information

Geometrical parameters for the optimized ground state for molecules **1**–**9** (Tables S1–S4); Atomic charges obtained by using NBO analysis (Table S5). This material is available free of charge on the Web at: http://www.csj.jp/journals/bcsj/.

References

1 R. K. Khanna, M. H. Moore, *Spectrochim. Acta, Part A* **1999**, *55*, 961.

2 W. W. Cleland, T. J. Andrews, S. Gutteridge, F. C. Hartman, G. H. Lorimer, *Chem. Rev.* **1998**, *98*, 549.

3 B. R. Ramachandran, A. M. Halpern, E. D. Glendening, *J. Phys. Chem. A* **1998**, *102*, 3934.

4 R. L. Baron, *Environ. Health Perspect. Suppl.* **1994**, *S11*, 102.

5 M. A. Casadei, F. M. M. G. Zappia, *J. Org. Chem.* **1997**, *62*, 6754.

6 C. Safak, M. Erdogan, M. Erantan, R. Sunal, *Arch. Pharamacol.* **1988**, *321*, 859.

7 E. Angeles, S. Diaz-Barriga, A. E. Ordaz, L. M. E. Reyes, R. A. R. Herandez, A. Ramirez, A. M. de la Garza, A. M. Arriaga, E. Jimenez-Cardoso, R. L. Castanares, XVIIIth International Symposium on Medicinal Chemistry, **2004**.

8 M. Duca, P. B. Arimondo, S. Leonce, A. Pierre, B. Pfeiffer, C. Monneret, D. Dauzonne, *Org. Biomol. Chem.* **2005**, *3*, 1074.

9 G. Tarzia, A. Duranti, A. Tontini, G. Piersanti, M. Mor, S. Rivara, P. V. Plazzi, C. Park, S. Katuria, D. Piomelli, *J. Med. Chem.* **2003**, *46*, 2352.

10 A. G. Atanasov, S. Tam, J. M. Rocken, M. E. Baker, A. Odermatt, *Biochem. Biophys. Res. Commun.* **2003**, *308*, 257.

11 E. Humeres, N. A. Debacher, M. M. S. Sierra, *J. Org. Chem.* **1999**, *64*, 1807.

12 K. Steenland, L. Cedillo, J. Tucker, C. Hines, K. Sorensen, J. DEddens, V. Cruz, *Environ. Health Perspect.* **1997**, 105.

13 K. Iwata, T. Yamashita, H. Uehara, *Antimicrob. Agents Chemother.* **1989**, *33*, 2118.

14 E. Gaudernak, J. Seipelt, A. Triendl, A. Grassauer, E. Kuechler, *J. Virol.* **2002**, *76*, 6004.

15 J. Aradones, C. L. Rodriguez, A. Corbi, P. G. del Arco, M. Lopez-Cabrera, M. O. de Landazuri, J. M. Redondo, *J. Biol. Chem.* **1996**, *271*, 10924.

16 R. Schreck, R. Grassmann, B. Fleckenstein, P. A. Baeuerle, *J. Virol.* **1992**, *66*, 6288.

17 S. Martinez, P. G. Arco, A. L. Armeslla, J. Aramburu, C. Luo, A. Rao, J. M. Redondo, *Mol. Cell. Biol.* **1997**, *17*, 6437.

18 M. Hellmuth, C. Wetzler, M. Nold, J. H. Chang, S. Frank, J. Pfeilschifter, H. Muhl, *Carcinogenesis* **2002**, *23*, 1273.

19 N. Segovia, G. Crovetto, P. Lardelli, M. Espigares, *J. Toxicol.* **2002**, *22*, 353.

20 D. Li, S. Wang, Y. Ito, J. Zhang, C. Wu, *Acta Pharmacol. Sinica* **2005**, *26*, 359.

21 M. Koketsu, M. Ishida, N. Takakuro, H. Ishihara, *J. Org. Chem.* **2002**, *67*, 486.

22 H. Takahashi, A. Nishina, R. Fukumoto, H. Kimura, M. Koketsu, H. Ishihara, *Eur. J. Pharm. Sci.* **2004**, *24*, 291.

23 B. K. Barlow, M. J. Thiruchelvam, L. Bennice, D. A. Cory-Slechta, N. Ballatori, E. K. Richfield, *J. Neurochem.* **2003**, *85*, 1075.

24 C. W. Nogueria, G. Zeni, B. T. Rocha, *Chem. Rev.* **2004**, *104*, 6255.

25 D. Kaur, P. Sharma, P. V. Bharatam, N. Dogra, *THEOCHEM*, in press.

26 C. Hillebrand, M. Mlessinger, M. Eckert-Maksic, Z. B. Maksic, *J. Phys. Chem.* **1996**, *100*, 9698.

27 P. Li, Y. Bu, H. Ai, Z. Cao, *J. Phys. Chem. A* **2004**, *108*, 4069.

28 M. J. Frisch, G. W. Trucks, H. B. Schiegel, G. E. Scuseria, M. A. Robb, J. R. Cheeseman, V. G. Zakrzewski, J. A. Montgomery, R. E. Stratmann, J. C. Burant, S. Dapprich, J. M. Millam, A. D. Daniels, K. N. Kudin, M. C. Strain, O. Farkas, J. Tomasi, V. Barone, M. Cossi, R. Cammi, B. Mennucci, C. Pomelli, C. Adamo, S. Clifford, J. Ochterski, G. A. Peterson, P. Y. Ayala, Q. Cui, K. Morokuma, D. K. Malick, A. D. Rubuck, K. Raghavchari, J. B. Foresman, J. Cioslowski, J. V. Oritz, B. B. Stefanov, G. Liu, A. Liashenko, P. Piskorz, I. Komaromi, R. Gomperts, R. L. Martin, D. L. Fox, T. Keith, M. A. Al-Laham, C. Y. Peng, A. Nanayakkara, C. Gonzalez, M. Challacombe, P. M. W. Gill, B. G. Jhonson, W. Chen, M. W. Wong, J. L. Andres, M. H. Gordon, E. S. Replogle, J. A. Pople, *Gaussian 98, Revision-A.11.2*, Gaussian Inc., Pittsburgh, PA, **1998**.

29 A. P. Scott, L. Radom, *J. Phys. Chem.* **1996**, *100*, 16502.

30 M. Remko, B. M. Rode, *J. Phys. Chem. A* **1999**, *103*, 431.

31 J. E. Carpenter, F. Weinhold, *THEOCHEM* **1988**, *169*, 41.

32 A. E. Reed, L. A. Curtiss, F. Weinhold, *Chem. Rev.* **1988**, *88*, 899.

33 M. Aresta, D. B. Tkatchenko, D. B. D. Amico, M. C. Bonnet, D. Bosch, F. Claderazzo, R. Fauri, L. Labella, F. Marchetti, *Chem. Commun.* **2000**, 1099.

34 H. Egsgaard, L. Carleson, *J. Chem. Soc., Faraday Trans.* **1994**, *90*, 886.

35 P. Politzer, J. E. Huheey, J. S. Murray, M. Grodzicki, *THEOCHEM* **1992**, *259*, 99.

36 G. N. Merrill, S. R. Kass, *J. Phys. Chem.* **1996**, *100*, 17465.

37 B. J. Smith, L. Radom, *J. Am. Chem. Soc.* **1993**, *115*, 4885.

38 K. Masuda, Y. Ito, M. Horiguchi, H. Fujita, *Tetrahedron* **2005**, *61*, 213.

39 D. M. Rudkevich, H. J. Xu, *J. Chem. Soc.* **2005**, 2651.